PROCEEDINGS OF SCIENCE

J/ψ production in pp and heavy-ion collisions at ATLAS

Shih-Chieh Hsu*
For the ATLAS Collaboration
Lawrence Berkeley National Lab
E-mail: schsu@cern.ch

The inclusive production of the J/ψ meson in its dimuon decay mode is studied in proton-proton collisions at center-of-mass energy 7 TeV with 2.4 pb^{-1} data accumulated by the ATLAS experiment at the LHC during April to August 2010 operation. The double differential cross section is measured with respect to the transverse momentum and rapidity of the J/ψ. The fraction of J/ψ mesons produced from B-hadron decays is also measured as a function of J/ψ transverse momentum and rapidity, and is used to determine the differential cross section for prompt and non-prompt J/Psi, separately. The centrality-dependent suppression in the yield of J/ψ dimuons together with an observation of Z boson production in collisions of lead-lead runs at a nucleon-nucleon center of mass energy 2.76 TeV, corresponding to an integrated luminosity of 6.7 μb^{-1} accumulated in Nov 2010, are discussed.

The 13th International Conference on B-Physics at Hadron Machines - Beauty2011,
April 04-08, 2011
Amsterdam, The Netherlands

*Speaker.

PoS(BEAUTY 2011)028

1. Introduction

The production of quarkonium in hadronic collisions can help the understanding of a unified mechanism, not found yet, that can consistently explain the J/ψ production in e^+e^-, heavy-ion and hadron-hadron collisions [1]. This proceedings presents a measurement of the inclusive J/ψ production cross-section and the production fraction f_B of non-prompt J/ψ (produced via the decay of a B-hadron) to inclusively-produced J/ψ in the decay channel $J/\psi \to \mu^+\mu^-$ as a function of both J/ψ transverse momentum and rapidity in pp collisions at the LHC at a centre-of-mass energy of 7 TeV and with an integrated luminosity of up to 2.3 pb^{-1}. From these measurements, the prompt J/ψ production cross-section produced directly from the proton-proton collisions or from decays of heavier charmonium states like the χ_c or $\psi(2S)$) are extracted. The non-prompt J/ψ production cross-section is presented in [2]. Measurements of the relative yields of J/ψ meson and Z boson in the dimuon final state as a function of centrality in lead-lead collisions at a nucleon-nucleon center of mass energy of $\sqrt{s_{NN}} = 2.76$ TeV with an integrated luminosity $\sim 6.7\ \mu$b^{-1} are also reported. More details of these measurements can be found in [3, 4].

2. Detector

Muons are measured by combining independent measurements of the muon trajectories from the Inner Detector (ID) and the Muon Spectrometer (MS). A detailed description of these detectors and their performance in proton-proton collisions can be found in Refs. [5]. The ID volume is within the 2 T field of a superconducting solenoid, and measures the trajectories of charged particles in the pseudorapidity region $|\eta| < 2.5$ The momentum scale measured in the ID is accurate to about 0.1% at low energy and about 1% up to 100 GeV, where alignment becomes the dominant effect. The primary-vertex resolution is O(10 μm). The MS is located inside a toroidal magnetic field which provides 2.5 Tm of bending power in the barrel and 5 Tm in the end-caps. The muon reconstruction efficiency is ranged from 82% to 100% in different transverse momentum, η and ϕ region and the fake rate is $\sim 0.1\%$. Both of them are measured with data-driven methods. Relative momentum resolution of combined muon ranges from about 2% at low momentum up to about 3% at $p_{\mathrm{T}} \sim 50$ GeV. For details about the muon reconstruction and its performance, see [6]. Two types of muon tracks are reconstructed: the combined muons, which take information from the ID and MS into one refitted muon track, and the tagged muons, which take an ID track and match it to hits in the MS. Both types of muons are used in pp collision analysis while only combined muons are used in the lead-lead collision analysis.

The ATLAS detector has a three-level trigger system: level 1 (L1), level 2 (L2) and the event filter (EF). For the measurements in pp collision, the trigger relies on the Minimum Bias Trigger Scintillators (MBTS) and the muon trigger chambers. For lead-lead collision, only MBTS trigger is used in the offline analysis.

Lead-lead collision centrality percentiles are defined from the total transverse energy, $\Sigma E_{\mathrm{T}}^{\mathrm{FCal}}$, measured in the forward calorimeter (FCal), which covers $3.2 < |\eta| < 4.9$. The full data sample is divided into four bins of collision centrality, 40-80%, 20-40%, 10-20%, and 0-10%. The most peripheral 20% of collisions are excluded from this analysis due to larger systematic uncertainties in estimating the number of binary nucleon-nucleon collisions in these events.

3. J/ψ production in proton-proton collisions

Events passing the trigger selection are required to have at least three tracks associated with the same reconstructed primary vertex to veto cosmics. J/ψ candidates require two opposite charged muons and at least one of which is a combined muon. The ID tracks associated to those muons are fitted to a secondary vertex and the opposite-charge di-muon invariant mass is recomputed. In order to recover the true number of J/ψ decaying to $\mu\mu$ produced in the collisions, a weight w is applied to each observed J/ψ candidate, defined as the inverse of the reconstruction probability $P = w^{-1} = \mathscr{A} \cdot \mathscr{M} \cdot \mathscr{E}^2_{\rm trk} \cdot \mathscr{E}^+{}_\mu(p_T^+, \eta^+) \cdot \mathscr{E}^-{}_\mu(p_T^-, \eta^-) \cdot \mathscr{E}_{\rm trig}$, where $\mathscr{A}$ is the kinematic acceptance, $\mathscr{M}$ is a correction factor for bin migrations due to finite detector resolution, $\mathscr{E}_{\rm trk}$ is the ID tracking efficiency for muons, $\mathscr{E}_\mu$ is the single-muon offline reconstruction efficiency and $\mathscr{E}_{\rm trig}$ is the di-muon candidate trigger efficiency.

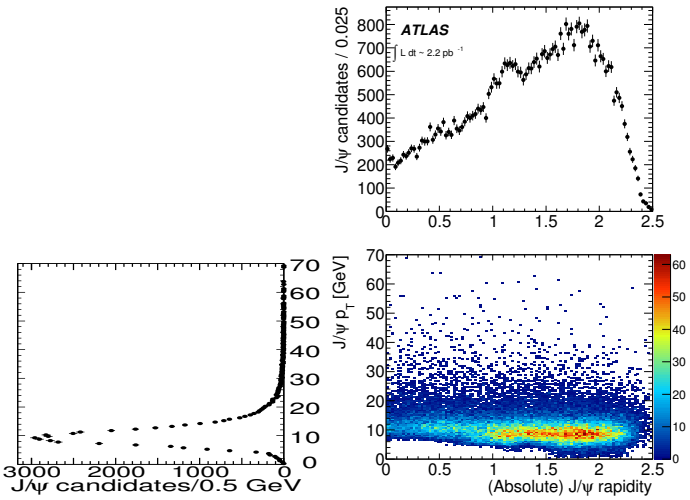

Figure 1: Distribution of reconstructed J/ψ candidates (in the invariant mass interval $2.7 < m_{J/\psi} < 3.5$ GeV) as a function of J/ψ p_T and rapidity [3].

Figure 1 shows the invariant mass distribution of the dimuons used in the cross section analysis and the J/ψ p_T and y in the signal mass region. The majority of J/ψ candidates are reconstructed in intermediate-p_T, high-y areas, as at lower p_T values the acceptance of the detector is limited. The inclusive J/ψ production cross-section is determined in four slices of J/ψ rapidity: $|y| < 0.75, 0.75 < |y| < 1.5, 1.5 < |y| < 2.0$ and $2.0 < |y| < 2.4$ and presented in Figure 2. The measurement in each $p_T - y$ analysis bin is positioned at the average p_T for J/ψ candidates in that bin. The spin alignment uncertainty calculated from maximal deviation of 5 spin-alignment scenarios is the largest uncertainty and regarded as theoretical uncertainties. The dominant measurement systematic uncertainty is from data-driven muon reconstruction efficiency uncertainties. The other systematics contribution ordered in size are trigger efficiency, luminosity, bin migration, final-state radiation and fitting method.

J/ψ from prompt production tends to decay very close to the primary vertex of the parent proton-proton collision, while many of the J/ψ mesons produced in B-hadron decays will have a measurably displaced decay point due to the long lifetime of their B-hadron parent. The signed projection of the J/ψ flight distance, $\vec{L}$, onto its transverse momentum, $\vec{p}_T^{\,J/\psi}$, is used to construct the displacement L_{xy} of the J/ψ vertex in the transverse plane via $L_{xy} \equiv \vec{L} \cdot \vec{p}_T^{\,J/\psi} / p_T^{J/\psi}$. Since the B-hadron is not fully reconstructed, a pseudo-proper time τ is constructed using J/ψ transverse

momentum through $\tau = \frac{L_{xy}\, m_{\rm PDG}^{J/\psi}}{p_T^{J/\psi}}$. A simultaneous unbinned maximum-likelihood fit is performed in di-muon mass and pseudo-proper time, in order to get the J/ψ mass and resolution, the J/ψ signal fraction, the non-prompt J/ψ fraction f_B and the pseudo-proper time slope and resolution. The world average value of $m_{\rm PDG}^{J/\psi}$ is used to reduce the correlation between the fits.

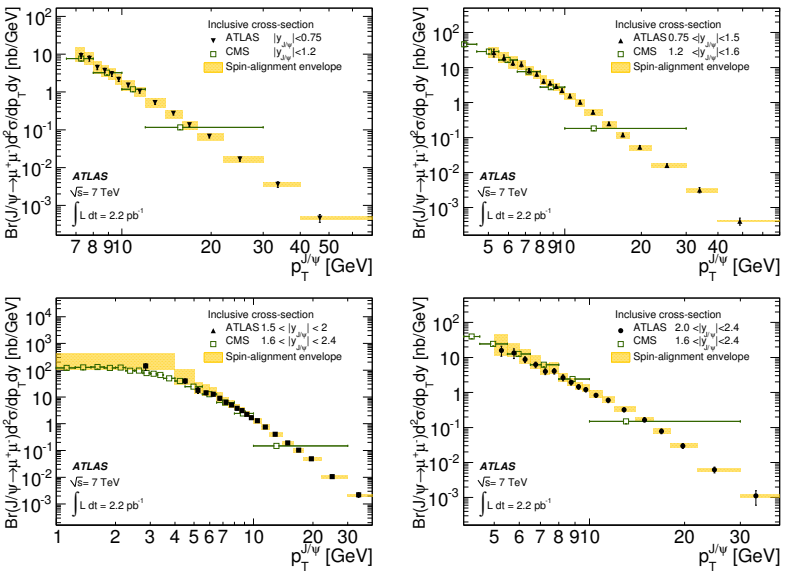

Figure 2: Inclusive J/ψ production cross-section as a function of J/ψ transverse momentum in the four rapidity bins. Overlaid is a band representing the variation of the result under various spin-alignment scenarios (see text) representing a theoretical uncertainty. The equivalent results from CMS [7] are overlaid. The luminosity uncertainty (3.4%) is not shown [3].

Figure 3 show the results of the differential non-prompt fraction measurement as a function of average $p_T^{J/\psi}$, in each of the four rapidity bins. The uncertainty envelopes due to the unknown spin-alignment are overlaid as solid bands. The ATLAS results exhibit good agreement with CMS [7] results where they overlap, and also with the CDF [8] measurements, indicating that there is no strong dependence of the fraction on collision energies. ATLAS further explores the high momentum regions as a complementary to CMS and CDF results.

Figure 4 shows the prompt production cross-section results extracted from inclusive cross-section and non-prompt fraction measurements and compared to the predictions of the Colour Evaporation Model (CEM) [9] and Colour Singlet Model (CSM) [10] at next-to-leading order (NLO) and a partial next-to-next-leading order calculation (NNLO*). NNLO* shows vast improvement over earlier LO predictions that are compared to Tevatron data, although these predictions still don't describe the full spectrum particularly at the highest transverse momenta explored in this analysis.

4. Di–muon production in lead-lead collisons

In the offline analysis, minimum-bias triggered events are required to have a reconstructed primary vertex, at least one hit in each set of MBTS counters, and a time difference between

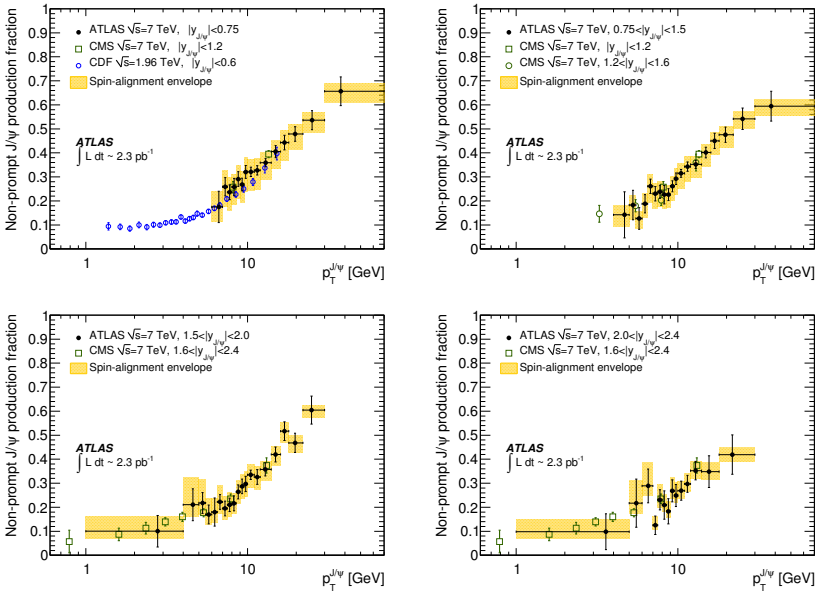

Figure 3: J/ψ non-prompt to inclusive fractions as a function of J/ψ transverse momentum. Overlaid is a band representing the variation of the result under various spin-alignment scenarios (see text) representing a theoretical uncertainty on the prompt and non-prompt J/ψ components. The equivalent results from CMS [7] and CDF [8] are included [3].

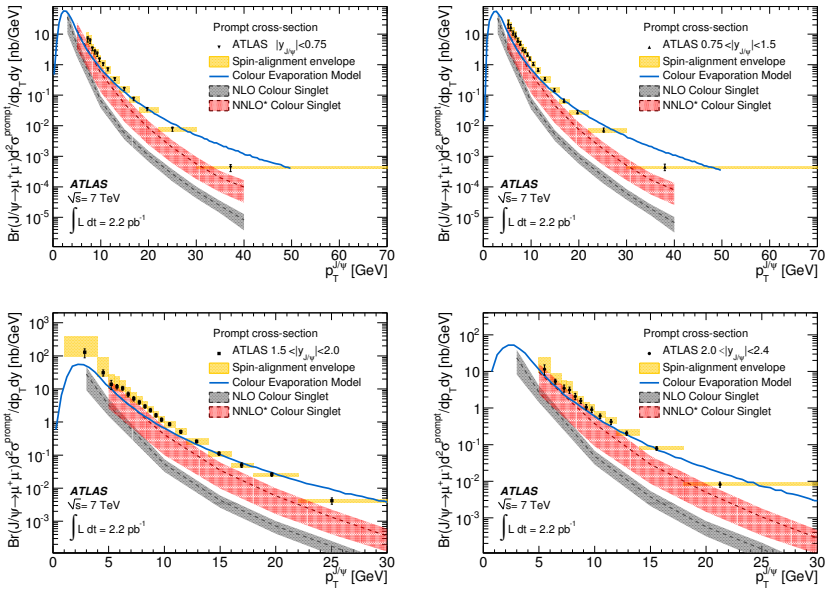

Figure 4: Prompt J/ψ production cross-section as a function of J/ψ transverse momentum in the four rapidity bins. Overlaid is a band representing the variation of the result under various spin-alignment scenarios (see text) representing a theoretical uncertainty on the prompt component. Predictions from NLO and NNLO* calculations, and the Colour Evaporation Model are overlaid. The luminosity uncertainty (3.4%) is not shown [3].

the sides of less than 3 ns to reject beam-halo and other beam-related background events. J/ψ candidates are selected from two oppositely charged combined muons with a minimum p_{T} of 3 GeV each and within the region $|\eta| < 2.5$. There is no selection cut on the transverse momentum of J/ψ candidates while 80% of the reconstructed J/ψ have $p_T > 6.5$ GeV.

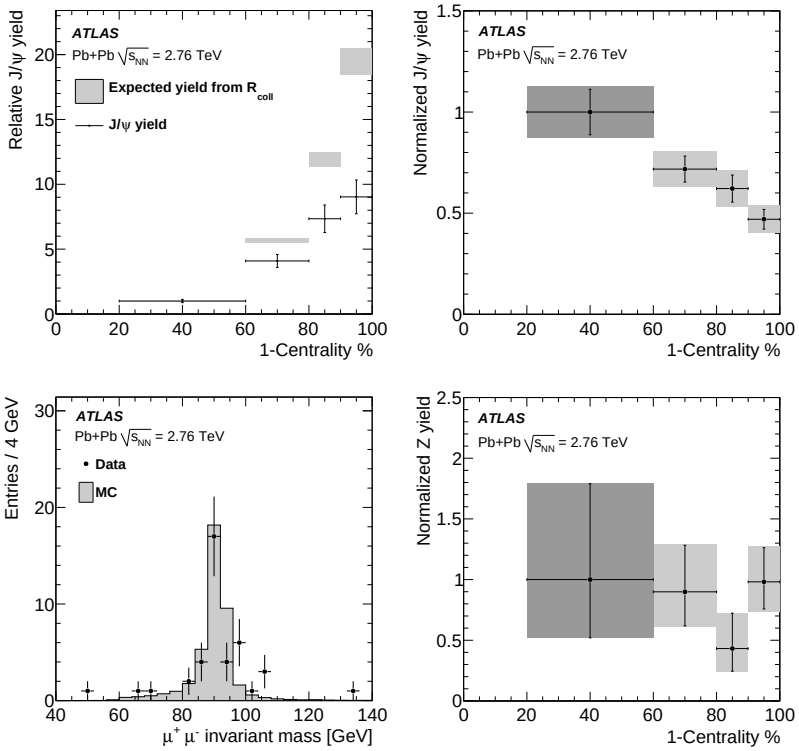

Figure 5: (top left) Relative J/ψ yield as a function of centrality normalized to the most peripheral bin (black dots with errors). The expected relative yields from the number of binary collisions (R_{coll}) are also shown. (top right) Value of R_{cp} of J/ψ. (bottom left) Di-muon invariant mass of Z candidates. (bottom right) Value of R_{cp} of Z. The statistical errors are shown as vertical bars while the grey boxes combining 1σ systematic errors. The darker box indicating the 40-80% bin is used to set the relative scale but the uncertainty is not propagated to the other bins [4].

The measured J/ψ yields at different centralities are corrected by the reconstruction efficiency ε_c for $J/\psi \to \mu^+\mu^-$, derived from MC and parameterized in each centrality bin, and the width of the centrality bin, W_c, which represents a well-defined fraction of the minimum bias events. The corrected yield of J/ψ mesons is given by: $N_c^{\mathrm{corr}}(J/\psi \to \mu^+\mu^-) = \frac{N^{\mathrm{meas}}(J/\psi \to \mu^+\mu^-)_c}{\varepsilon(J/\psi)_c \cdot W_c}$. The "relative yield" shown in the top left panel of Figure 5 is defined by normalizing to the yield found in the most peripheral 40-80% centrality bin: $R_c = N_c^{\mathrm{corr}}/N_{40-80\%}^{\mathrm{corr}}$. The uncertainties in the 40-80% bin are not propagated into this ratio for the more central bins. The normalized yield R_{cp} as shown in the top right panel of Figure 5 is defined by scaling the relative yield by the ratio R_{coll} of the mean number of binary collisions $N_{\mathrm{coll},c}$, calculated using a Glauber Monte Carlo package [11]. The data points are not consistent with their average, giving a $P(\chi^2, N_{\mathrm{DOF}})$ value of 0.11% with three degrees of freedom, computed conservatively ignoring any correlations among the systematic uncertainties. A significant decrease of R_{cp} as a function of centrality is observed to be compared

to previous low energy experiments [12].

Z candidates are selected by requiring a pair of oppositely charged muons with $p_{\mathrm{T}} > 20$ GeV and $|\eta| < 2.5$. An additional cosmic ray rejection cut on the sum of the pseudorapidities of the two muons, $|\eta_1 + \eta_2| > 0.01$, is also applied. The invariant mass distribution of 38 Z candidates is displayed in the bottom left panel of Figure 5. Within the large statistical uncertainty, no strong statement could be drawn from the centrality dependence of R_{cp} in the bottom right panel of Figure 5.

5. Summary

Results are presented on the measurement of the inclusive cross-section, non-prompt fraction and the prompt cross-section of $J/\psi \to \mu^+\mu^-$ production in proton-proton collisions at a collision energy of 7 TeV using the ATLAS detector at the LHC with up to 2.3 pb^{-1} of integrated luminosity. It is found the measurements made by ATLAS, CMS and CDF in those overlapping regions are in a good agreement. The theoretical curves show significant deviations in the prompt production spectra both in shape and normalization, particularly at high transverse momenta, while theoretical descriptions show a better agreement to the non-prompt production cross-section of J/ψ [3]. A centrality dependent suppression in the normalized J/ψ yield together with the first Z boson observation in lead-lead collisions at nucleon center of mass energy 2.76 TeV are reported.

References

[1] M. Kramer, Prog. Part. Nucl. Phys. **47** (2001) 141; J. P. Lansberg, Int. J. Mod. Phys. A **21** (2006) 3857; J. P. Lansberg *et al.*, AIP Conf. Proc. **1038** (2008) 15; T. Matsui and H. Satz, Phys. Lett. **B178** (1986) 416; A. Mocsy and P. Petreczky, Phys. Rev. Lett. **99** (2007) 211602.

[2] I. A. Christidi,*Open b and bb cross-section measurements using inclusive and exclusive channels at ATLAS, in these proceedings.*

[3] ATLAS Collaboration, Nucl. Phys. B **850**, 387 (2011).

[4] ATLAS Collaboration, Phys. Lett. B **697**, 294 (2011).

[5] ATLAS Collaboration, JINST **3** (2008) S08003.

[6] M. Corradi, *Di-muon Reconstruction for B-physics in ATLAS, in these proceedings.*

[7] CMS Collaboration, Eur. Phys. J. C **71**, 1575 (2011).

[8] CDF Collaboration, T. Aaltonen et al., Phys. Rev. **D71** (2005) 032001.

[9] T. Ullrich, A. D. Frawley and R. Vogt, Phys. Rept. **462** (2008) 125; V. D. Barger, W. Y. Keung and R. J. N. Phillips, Phys. Lett. B **91** (1980) 253; V. D. Barger, W. Y. Keung and R. J. N. Phillips, Z. Phys. C **6** (1980) 169.

[10] J. Lansberg, arXiv:1006.2750 [hep-ph]; S. J. Brodsky and J. P. Lansberg, Phys. Rev. D **81** (2010) 051502; J. P. Lansberg, Eur. Phys. J. C **61** (2009) 693.

[11] B. Alver, M. Baker, C. Loizides *et al.*, arXiv:0805.4411 [nucl-ex]; M. L. Miller, K. Reygers, S. J. Sanders *et al.*, Ann. Rev. Nucl. Part. Sci. **57** (2007) 205-243.

[12] NA50 Collaboration, B. Alessandro *et al.*, Eur. Phys. J. **C39** (2005) 335-345. PHENIX Collaboration, A. Adare *et al.*, Phys. Rev. Lett. **98** (2007) 232301.